

# Cytotoxicity of cultured macrophages exposed to antimicrobial zinc oxide (ZnO) coatings on nanoporous aluminum oxide membranes

Peter E. Petrochenko,<sup>1,2</sup> Shelby A. Skoog,<sup>1,2</sup> Qin Zhang,<sup>1</sup> David J. Comstock,<sup>3</sup> Jeffrey W. Elam,<sup>3</sup> Peter L. Goering<sup>1</sup> and Roger J. Narayan<sup>2,\*</sup>

<sup>1</sup>Division of Biology; Office of Science and Engineering Laboratories; Center for Devices and Radiological Health; U.S. Food and Drug Administration; Silver Spring, MD USA; <sup>2</sup>Joint Department of Biomedical Engineering; UNC—Chapel Hill and North Carolina State University; Raleigh, NC USA; <sup>3</sup>Energy Systems Division; Argonne National Laboratory; Argonne, IL USA

**Keywords:** anodic aluminum oxide, atomic layer deposition, nanoporous materials, zinc oxide, macrophage, cytotoxicity, reactive oxygen species (ROS)

Zinc oxide (ZnO) is a widely used commercial material that is finding use in wound healing applications due to its antimicrobial properties. Our study demonstrates a novel approach for coating ZnO with precise thickness control onto 20 nm and 100 nm pore diameter anodized aluminum oxide using atomic layer deposition (ALD). ZnO was deposited throughout the nanoporous structure of the anodized aluminum oxide membranes. An 8 nm-thick coating of ZnO, previously noted to have antimicrobial properties, was cytotoxic to cultured macrophages. After 48 h, ZnO-coated 20 nm and 100 nm pore anodized aluminum oxide significantly decreased cell viability by  $\approx 65\%$  and  $54\%$ , respectively, compared with cells grown on uncoated anodized aluminum oxide membranes and cells grown on tissue culture plates. Pore diameter (20–200 nm) did not influence cell viability.

## Introduction

Zinc oxide (ZnO) is a widely utilized commercial material that has recently garnered interest by medical and nanotechnology researchers due to its considerable antimicrobial<sup>1</sup> and UV protection properties.<sup>2</sup> In a review by Lansdown et al., the authors emphasize the importance of numerous Zn materials that have good clinical evidence showing anti-infective activity, improved wound healing, and higher epithelialization rates.<sup>3</sup> A large number of commercial materials use ZnO as an active component, such as bandages, stockings, and occlusive adhesive dressings.<sup>3</sup> Nanoscale forms of ZnO have been considered for use in nontoxic antimicrobial wound dressings.<sup>4</sup> In addition, discrete ZnO nanoparticles have been shown to exhibit strong antimicrobial activity against Gram-positive bacteria<sup>5,6</sup> as well as some preferential toxicity toward cancerous human myeloblastic leukemia cells (HL60) when compared with normal peripheral blood mononuclear cells.<sup>6</sup> There could be several reasons for preferential cell toxicity; one potential mechanism for this behavior (e.g., for ZnO nanoparticle toxicity) may involve the generation of reactive oxygen species (ROS).<sup>6</sup> ROS generation, however, is generally assumed to occur after cellular uptake of Zn ions.<sup>7</sup> ZnO nanoparticles themselves produce little ROS but generate dissolved Zn<sup>2+</sup> ions, which then enter the cell and cause production of intracellular ROS.<sup>7</sup>

Both ionic Zn and ZnO nanomaterials have been shown to decrease cell viability in several mammalian cell lines. Various cells of the immune system, for example, respond differently to ZnO nanomaterials. For example, monocyte-derived dendritic cells exhibit a dose-dependent cytotoxic response and an increase in the activity of caspases, enzymes which are involved in apoptotic cell death; however, peripheral blood mononuclear cells are not affected.<sup>8</sup> At sub-cytotoxic concentrations, ZnO may modulate immune responses in some immune cell types but not others.<sup>8</sup> In general, the mode of toxicity for ZnO nanomaterials is thought to involve free Zn ions and likely follows a classical dose and time-dependent response for intracellular ROS production and cytotoxicity.<sup>9</sup>

ZnO has been shown to be toxic in vivo via certain routes of exposure. For example, ZnO nanoparticles were noted to be more toxic to the lungs than the equivalent dose in ionic (ZnCl<sub>2</sub>) form following intratracheal instillation.<sup>10</sup> The particles are thought to be trapped in the lung and continuously release Zn ions that cause toxicity; the ionic solution is cleared more easily.<sup>10</sup> When incorporated into hydrogel wound dressing bandages, ZnO nanomaterials impart improved healing and antimicrobial activity.<sup>11</sup> Nano-scale ZnO shows good in vivo outcomes in dermatology applications such as sunscreens and cosmetics, where it has limited penetration into skin layers and has little or

\*Correspondence to: Roger J. Narayan; Email: roger\_narayan@msn.com

Submitted: 05/27/13; Accepted: 06/25/13

Citation: Petrochenko PE, Skoog SA, Zhang Q, Comstock DJ, Elam JW, Goering PL, et al. Cytotoxicity of cultured macrophages exposed to antimicrobial zinc oxide (ZnO) coatings on nanoporous aluminum oxide membranes; Biomatter 2013; 3:e25528; <http://dx.doi.org/10.4161/biomatter.25528>

no effect on skin cell activity (e.g., morphology, metabolism or oxidation).<sup>12</sup>

When compared with discrete nanoparticles, very little toxicology literature is available on nanotextured surfaces.<sup>13</sup> Similar features are present in discrete nanoparticles and on nanotextured surfaces, namely the relatively large surface area and high radius of curvature inherent to nanoscale features. ZnO can be coated onto nanotextured surfaces without disrupting the underlying surface morphology using a thin film growth process known as atomic layer deposition (ALD). A ZnO-coated nanotextured surface will have a greater surface area for cell interactions than a smooth surface;<sup>14</sup> as such, the ZnO-coated nanotextured surface may exhibit a higher rate of Zn ion dissolution. Skoog et al. previously demonstrated that ZnO-coated anodized aluminum oxide membranes exhibit antimicrobial activity against several bacterial strains associated with skin infection; significant activity against Gram-positive bacteria was noted.<sup>15</sup> They showed that membranes with ALD-grown ZnO coatings leach Zn ions in vitro. The extract from the ZnO-coated 20 nm and 100 nm anodized aluminum oxide membranes contained Zn at a concentration of approximately 90 µg/ml.<sup>16</sup> This study raised the question about the cytotoxic potential of the released Zn ions to eukaryotic cells. The objective of the present study was to evaluate macrophage responses (e.g., cytotoxicity and ROS production) of an ALD-grown ZnO coating on an anodized aluminum oxide substrate. The underlying inert substrate used in the study was anodized aluminum oxide, which is known to have good cell adhesion and proliferation in vitro compared with a standard tissue culture well. Hoess et al. showed that cells interact with 200 nm pores and thus may exhibit different responses to membranes with dissimilar pore diameters.<sup>16</sup> Ferraz et al. indicated that differences in nanoporosity elicited dissimilar immune responses for 20 and 200 nm diameter anodized aluminum oxide in vivo.<sup>17</sup> In this study, cellular responses to ZnO-coated and uncoated 20 nm and 100 nm anodized aluminum oxide membranes were evaluated using the MTT cell viability assay and the ROS production assay.

## Results

**Surface characterization.** Scanning electron microscopy was performed to examine the morphologies of the coated and uncoated nanoporous anodized aluminum oxide membranes. All of the membranes had one side with circular 200 nm diameter pores [designated as Side A (Fig. 1A and B)], which narrowed to either 20 nm or 100 nm diameter branched pores on the other side (designated as Side B). Side B scanning electron micrographs for the 100 nm uncoated and ZnO-coated anodized aluminum oxide membranes are shown in Figures 1C and D, respectively. Figures 1B and D are representative SEM images of the coated membranes; artifacts (e.g., crystals) resulting from the deposition process were noted on the surfaces of the coated membranes. The crystals were noted in images that were obtained from cleaved cross-sectional specimens (Fig. 2A). The majority of the coated membrane surface was free of these crystals. The pores were noted to continue from one side of the

membrane to the other. To determine whether the ALD precursors penetrated through the entire membrane, EDX elemental analysis was used to evaluate Side A, Side B, and the center of the membrane; as noted in the gold text of Figure 2A, ZnO was shown to be present in each of these three regions of the nanoporous structure (shown). Figure 2B shows a representative EDX spectrum of the 200 nm pore side (Side A) of a ZnO-coated anodized aluminum oxide membrane. Prominent Zn and Al peaks were noted on spectra that were obtained from throughout the membrane.

**Cell responses.** No significant differences were noted in cell viability (MTT assay) after 24 h exposure to any coated or uncoated membrane (Fig. 3). The ZnO-coated nanoporous membranes trended toward lower viability values; however, the differences with tissue culture polystyrene plate controls (TCPS) after 24 h were not statistically significant. Cells exposed to ZnO-coated 20 nm anodized aluminum oxide showed decreased viability; for example, viability of cells exposed to ZnO-coated anodized aluminum oxide was approximately 32% lower than that of cells grown in culture wells (TCPS). Viability of cells grown on ZnO-coated 100 nm anodized aluminum oxide was approximately 36% lower than that of cells grown in culture wells. After 48 h, cell viability for both ZnO-coated 20 nm anodized aluminum oxide and ZnO-coated 100 nm anodized aluminum oxide was significantly lower ( $P < 0.01$ ) than for the corresponding uncoated controls and TCPS controls. Cell viability for ZnO-coated 20 nm anodized aluminum oxide decreased by approximately 65% and ZnO-coated 100 nm anodized aluminum oxide decreased by approximately 54% from controls. Pore diameter did not appear to influence cell viability for coated or uncoated membranes. There were no differences among cell viability for 20, 100, or 200 nm pore diameter membranes after both 24 and 48 h (the data for the 200 nm pore surface not included on MTT figure). Moreover, the anodized aluminum oxide substrates themselves did not affect cell viability.

Production of intracellular ROS was monitored from 1 to 24 h after treatment using extracts collected from incubating ZnO-coated membranes for 24 h (Fig. 4). No significant increases in ROS production were observed between any groups at each time point. The H<sub>2</sub>O<sub>2</sub> positive control induced a very strong response from the cells; in addition, no interference with the dye was observed.

## Discussion

Several techniques are available for depositing ZnO coatings onto anodized aluminum oxide membranes, including pulsed laser deposition (PLD),<sup>18</sup> ion beam sputtering,<sup>19</sup> plasma chemical vapor deposition (CVD),<sup>20</sup> and spin coating.<sup>21</sup> ALD has previously been used to deposit nanometer-thick coatings of ZnO on polymer nanofibers with no alteration to the underlying nanofiber structure.<sup>22</sup> Cross-sectional SEM/EDX analysis revealed a benefit of using ALD for growth of coatings on nanotextured surfaces, including nanoporous surfaces. The EDX data shown in Figure 2B indicates that ZnO was deposited throughout the surfaces of the nanoscale pores. The main benefit of ALD is its ability to

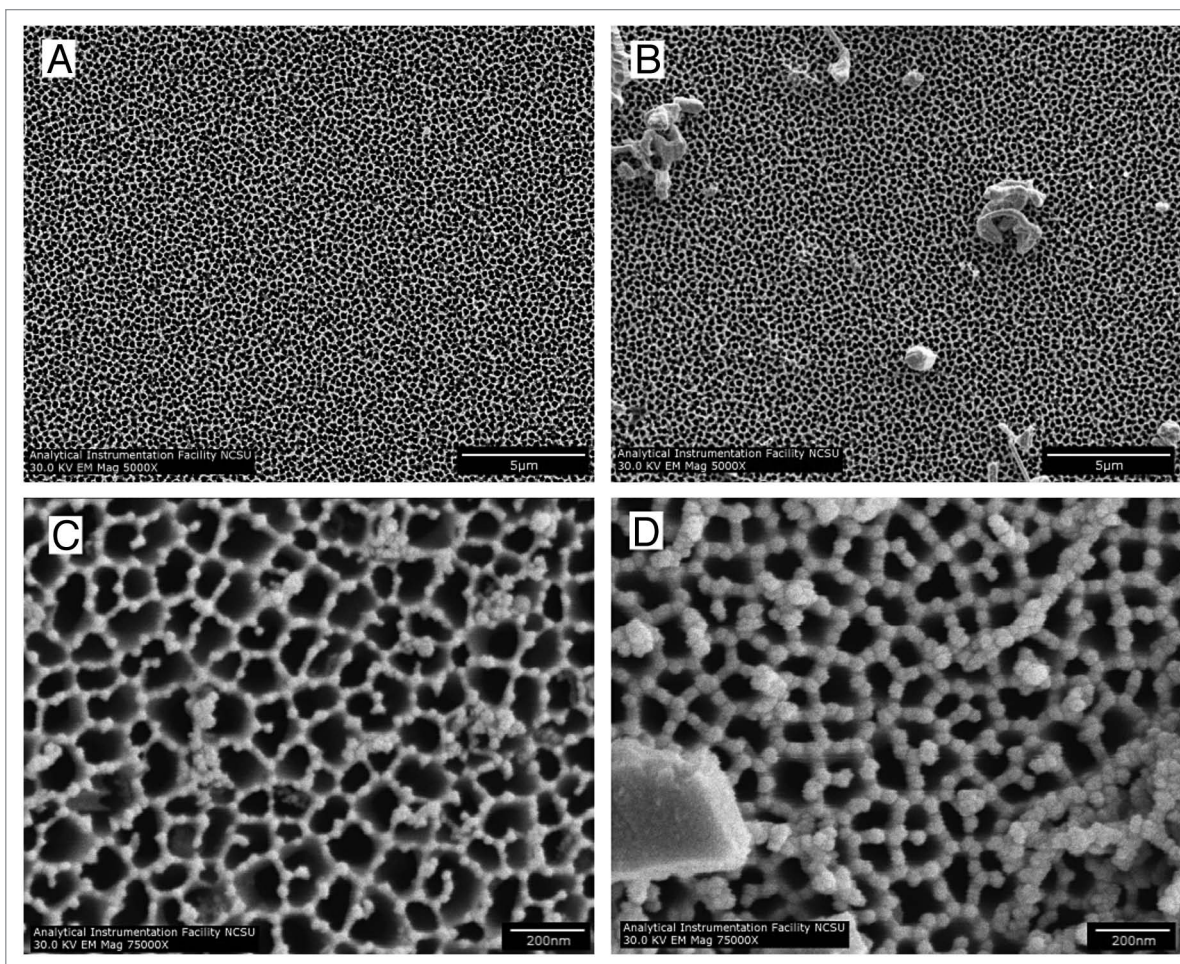


**Figure 1.** SEM images of both sides of a 100 nm anodized aluminum oxide membrane. (A) Side A of an uncoated anodized aluminum oxide membrane, showing 200 nm circular pores. (B) Side A of an 8 nm ZnO-coated anodized aluminum oxide membrane, showing 200 nm circular pores. (C) Side B of an uncoated anodized aluminum oxide membrane, showing 100 nm branching pores. (D) Side B of an 8 nm ZnO-coated anodized aluminum oxide membrane, showing 100 nm branching pores.

deposit conformal thin films over complex surface topographies. ALD is also particularly well suited for coating nanoporous anodized aluminum oxide materials and other materials with interconnected pores, which may be difficult to coat using other techniques.

In previous work, Palomaki et al. showed that ZnO nanoparticles elicited concentration-dependent cytotoxicity in RAW 264.7 macrophages.<sup>23</sup> The present study was aimed to determine whether cell viability can be affected by atomic layer deposition-grown ZnO-coated nanoporous surfaces instead of by free ZnO nanoparticles. Previous studies have indicated that the pore size of nanoporous anodized aluminum oxide membranes and coated membranes does not have a significant effect on cell viability.<sup>24</sup> As noted in the introduction, our group quantified Zn ion release from 20 nm and 100 nm anodized aluminum oxide membranes with atomic layer-deposition grown 8 nm-thick ZnO coatings into DMEM culture media containing 10% fetal bovine serum by means of inductively coupled plasma mass spectrometry.<sup>16</sup> This study confirms that varying the pore size between 20 and 200 nm does not alter cell viability as measured by the MTT assay.

Atomic layer deposition enables the amount of coating material that is deposited on the surface and subsequently released during use to be readily controlled. This attribute of atomic layer deposition is beneficial for coating medical devices with materials such as silver or zinc oxide, which are thought to produce antimicrobial activity through ionic interactions.<sup>25,26</sup>

The commercially-available nanoporous anodized aluminum oxide membranes used in this study are anisotropic; one side contains isolated, circular pores with a diameter of ~200 nm (Fig. 1A and B) and the other side contains a “branchlike” structure in which the pore diameter is ~20 or ~100 nm (Fig. 1C and D). Some crystals were noted on the surface of the 8 nm thick ZnO coating (Figs. 1 and 2); ZnO crystals may form on the membrane surface due to insufficient precursor purging between exposures. Some contamination by adventitious dust particles may also be present. It should be noted that the majority of the surface area of the ZnO-coated membrane was free of these crystals (Fig. 1B). The EDX elemental analysis showed Zn and Al peaks, which are attributed to the 8 nm thick ZnO coating and the underlying aluminum oxide substrate, respectively.

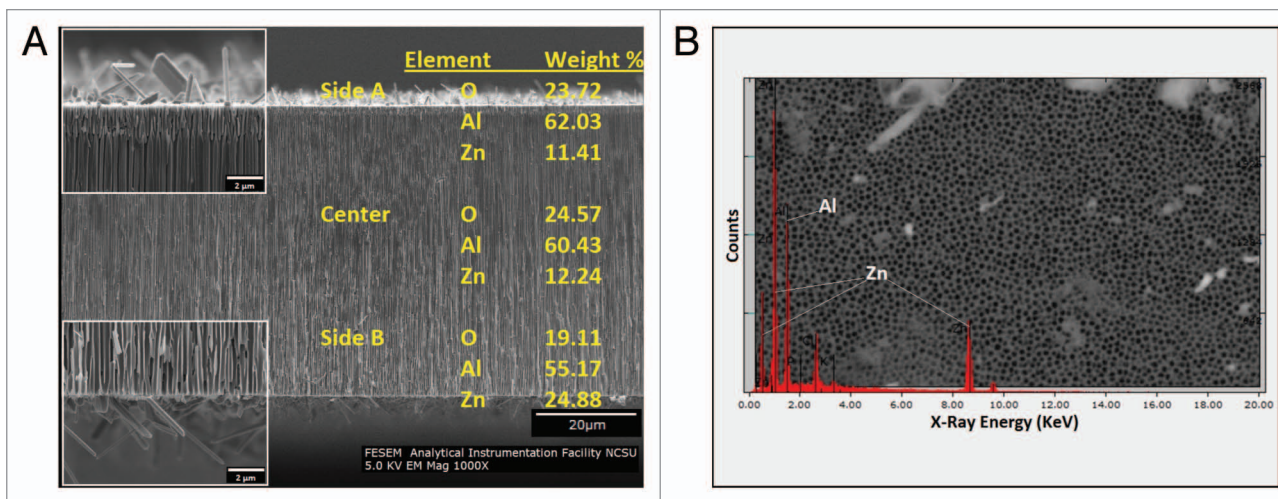


**Figure 2.** Cross-sectional SEM and elemental analysis of a 20 nm nanoporous anodized aluminum oxide with an 8 nm ZnO coating. **(A)** Cross-sectional view of the membrane, showing the crystals present on the surface. **(B)** EDX spectrum obtained from the 200 nm circular pore side, showing Al and Zn peaks (Side B).

The ZnO-coated membranes examined in this study were previously shown to possess antibacterial activity;<sup>16</sup> however, the cytotoxicity of these materials was not previously examined. It is evident from the MTT cell viability assay results that the ZnO-coated membranes are cytotoxic to macrophages after 48 h of incubation. No cytotoxicity was evident after 24 h, which suggests that there is a gradual release of Zn ions into the media over time. In addition, the data suggests that the effect of Zn ions on macrophages may be time-dependent. Zn ions are known to be toxic to a variety of cell types.<sup>27</sup> Many studies measure administration of a single bolus dose; toxicity results may differ if an identical dose is gradually administered over a period of time.

Cell culture methods also apparently have an effect on cell responses to ZnO; for example, keeping cell number and Zn concentration constant, more densely packed monolayers have higher resistance to Zn toxicity than an identical number of cells located further apart from one another.<sup>28</sup> The observed relationship between toxicity and seeding density is not fully understood and could occur due to differences in cellular function between isolated cells and cell assemblages. In the present study, cells are dispersed on the surfaces so that they are not directly touching each other, which could make them more susceptible to Zn ion toxicity.

Ionic zinc is known to modulate immune response from monocytes by suppressing TNF- $\alpha$  transcription and secretion.<sup>29</sup> For example, Grandjean-Laquerriere et al. showed that zinc decreases TNF- $\alpha$  production by unstimulated human monocytes.<sup>30</sup> Several previous studies have indicated that Zn prevents free radical generation and oxidative stress. In a rat model, Zn has been shown to decrease carbon tetrachloride-induced liver damage<sup>31</sup> from reactive free radical metabolites and reduce the toxicity of cadmium,<sup>32</sup> a known carcinogen. In mice, oral Zn administration decreased alcohol-induced liver damage<sup>33</sup> and toxicity from whole body radiation.<sup>34</sup> Rostan et al. considered the role of Zn as an antioxidant and discussed mechanisms in which redox stable

Zn may replace redox reactive metals such as iron and copper as well as function as a sacrificial site for oxidant attacks.<sup>35</sup> It should be noted that the amount of Zn ions in the extract may have not been sufficient to result in measurable production of ROS. Since the ZnO surfaces were toxic only after 48 h, it is possible that the amount of Zn that had leached out after 24 h was not sufficient to cause measurable production of ROS.

## Materials and Methods

**ZnO deposition.** Anodized aluminum oxide membranes with 20 nm pores and 100 nm pores were acquired from a commercial source (General Electric Healthcare). These membranes exhibited outside diameters of 13 mm and thicknesses of 60  $\mu\text{m}$ . The 20 nm pore size nanoporous anodized aluminum oxide membranes exhibited pore diameters of 200 nm for 58  $\mu\text{m}$  of the 60  $\mu\text{m}$  thickness and exhibited pore diameters of 20 nm for 2  $\mu\text{m}$  of the 60  $\mu\text{m}$  thickness. The 100 nm pore size nanoporous anodized aluminum oxide membranes exhibited pore diameters of 200 nm for: 58  $\mu\text{m}$  of the 60  $\mu\text{m}$  thickness and pore diameters of 100 nm for: 2  $\mu\text{m}$  of the 60  $\mu\text{m}$  thickness. The ZnO ALD was conducted at a pressure of  $\sim 1$  Torr using 360 sccm carrier gas flow of ultrahigh purity  $\text{N}_2$  in a custom viscous flow reactor. Prior to deposition, the nanoporous anodized aluminum oxide membranes were cleaned in situ by flowing ozone, which was generated by flowing 400 sccm ultrahigh purity  $\text{O}_2$  through a commercial ozone generator for five minutes at a temperature of 200°C. The ozone concentration generated using this approach was  $\sim 10\%$  and the ozone partial pressure was  $\sim 0.1$  Torr. ZnO was deposited on the surfaces of the membranes by iteratively exposing the membranes to diethylzinc (Sigma Aldrich) and water vapors at a deposition temperature of 200°C. For each precursor, a six second exposure at a partial pressure of  $\sim 0.2$  Torr was followed by a five second  $\text{N}_2$  purge. The anodized aluminum oxide membranes were coated with 8 nm ZnO as determined by

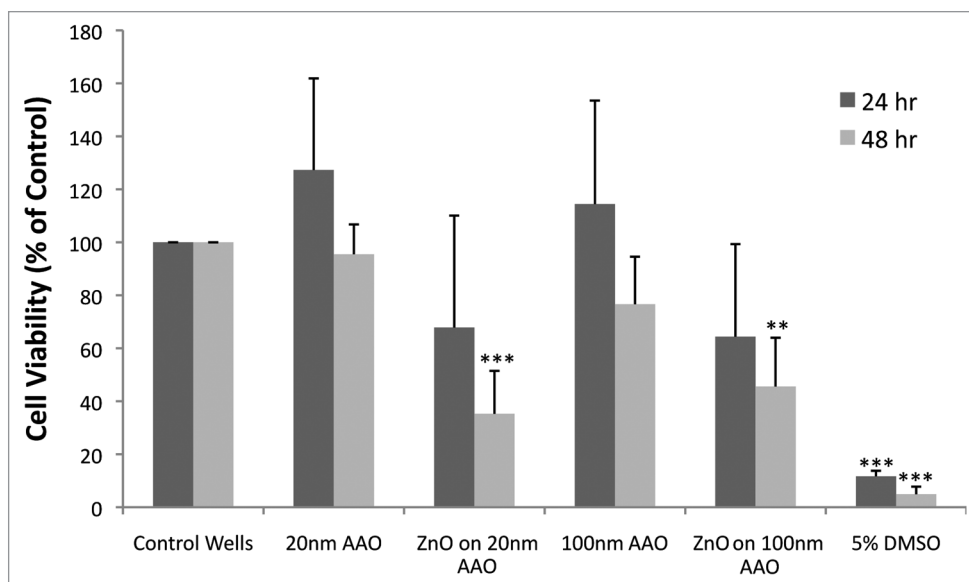


**Figure 3.** Cell viability (MTT assay) in macrophages cultured on nanoporous uncoated anodized aluminum oxide membranes and nanoporous Zn-coated anodized aluminum oxide membranes. No statistical differences are present at 24 h. After 48 h, cells cultured on both 20 and 100 nm ZnO-coated anodized aluminum oxide membranes showed a reduction in cell viability compared with cells cultured on corresponding uncoated anodized aluminum oxide membranes and cells grown on standard tissue culture wells. Statistical significance \*\*\* $P < 0.001$ , \*\* $P < 0.01$  from cell and media only control.

ellipsometry on Si(100) witness samples, which were concurrently coated with the anodized aluminum oxide membranes.

**Scanning electron microscopy.** Scanning electron microscopy (SEM) was performed using a JEOL 6400 cold field emission scanning electron microscope (JEOL). Energy dispersive X-ray spectroscopy (EDX) was performed in order to confirm the elemental composition of the surface. The SEM was equipped with an energy dispersive X-ray spectrometer attachment with a Link Pentafet detector (Link Analytical) and a 4Pi Universal Spectral Engine pulse processor (4Pi Analytical). An accelerated voltage of 20 keV was used in this study.

**MTT cell viability assay.** The annealed ZnO-coated nanoporous anodized aluminum oxide membranes and uncoated nanoporous anodized aluminum oxide membranes were assayed for potential cytotoxicity using the MTT [3-(4,5-dimethyl-2-thiazol)-2,5-diphenyl-2H-tetrazolium bromide] assay (CellTiter 96® non-radioactive cell proliferation assay) from a commercial source (Promega). Membranes were sterilized with UV light (UVP CL-1000). All membranes were

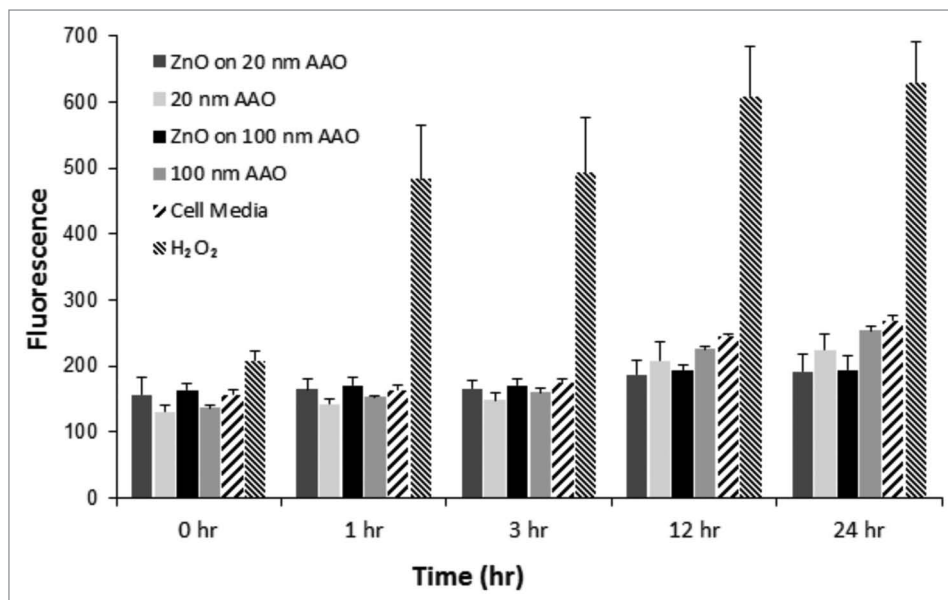


**Figure 4.** ROS production in macrophages treated with 24-h extracts from ZnO-coated anodized aluminum oxide membranes over 1 h, 3 h, 12 h, and 24 h. Cells were treated with H<sub>2</sub>O<sub>2</sub> as a positive control. All experimental groups, including ZnO-coated and uncoated anodized aluminum oxide, had similar responses to cells grown with fresh media, indicating no significant ROS generation for any surface extract.

exposed for two hours on each side and rotated 90° every 60 min to ensure complete sterilization. Upon completion of UV sterilization, the membranes were placed in 24-well plates. RAW 264.7 cells (mouse leukemic monocyte macrophage cell line),

which were obtained from a commercial source (ATCC), were added to the 24-well plates at a cell density of  $2 \times 10^5$  cells/mL in Dulbecco's Modified Eagle Medium (DMEM). All of the 24-well plates were incubated for either 24 h or 48 h. Following incubation, the membranes were moved to a new 24-well plate so that assays were conducted on cells grown only on the membranes and not in the non-membrane areas of the wells. The new wells contained 0.5 mL MTT-DMEM for macrophages. MTT-DMEM was prepared by adding MTT dye solution:medium at a 15:100 ratio as specified by the kit. A 75  $\mu$ l aliquot of MTT dye was added to each well in order to obtain a total volume of 0.5 ml. The plates were then incubated under cell culture conditions for 3 h. After each incubation period, the solubilization solution/stop mix was added and the plates were incubated again for 1 h at 37°C and 5% CO<sub>2</sub>. The wells were then mixed and the contents transferred to duplicate wells in a 96-well plate for absorbance measurements. Absorbance was measured at  $\lambda = 570$  nm (reference wavelength 650 nm) using a 96-well OPTIMax plate reader (Molecular Devices). Cells spiked with 5% and 10% dimethyl sulfoxide (DMSO) served as a positive control for the MTT assay. The data were normalized to the uncoated nanoporous anodized aluminum oxide membrane value and were expressed as percent viability.

**Reactive oxygen species (ROS) production assay.** The generation of intracellular ROS was measured by the increasing fluorescence of 2',7'-dichlorofluorescein (DCF). The cell-permeable 2',7'-dichlorodihydrofluorescein (DCF-DA) is oxidized by intracellular reactive oxygen species to the highly fluorescent dichlorofluorescein (DCF). Cells with a density of  $2 \times 10^5$  cells/mL ( $2 \times 10^4$  cells/well) were cultured in DMEM within a standard transparent 96-well plate overnight. After cells were washed twice with HBSS to remove culture medium, 5 mM DCF-DA in HBSS was added to all of the wells and the plate was incubated at 37°C for 30 min. After incubation, the DCF-DA reagent was removed and the cells were washed twice with HBSS. Different concentrations of ZnO extracts in 100  $\mu$ l aliquots of culture medium were added to each well. Cells were treated with 200  $\mu$ M hydrogen peroxide (H<sub>2</sub>O<sub>2</sub>) as a positive control. Different concentrations of extracts alone served as controls and were run in parallel to determine if there was any interference with the assay. DCF fluorescence was monitored after various treatments from 30 min to 24 h at excitation of 480 nm and emission of 530 nm using a fluorescence plate reader (Molecular Devices). Extracts were collected by placing sterilized filters into 24-well plates and incubating in 1 ml DMEM media at 37°C and 5% CO<sub>2</sub>. Wells with media but without membranes served as control extracts. Media was then removed after 24 or 48 h and was used for additional studies. ROS generation was obtained by measuring cells exposed to surface media extracts as opposed to measuring cells directly grown on various surfaces; this approach

with utilized in order to see if particulate or ionic leaching was the mode of toxicity as opposed to direct contact between the cells and the surface.

**Statistical analysis.** The results from each data set were analyzed with Prism 4 statistical software (GraphPad Inc.). The results were expressed as mean  $\pm$  standard deviation. Statistical differences between the control and treated group were assessed using a one-way ANOVA with a Bonferroni post hoc test. Each experiment was repeated at least three times with each sample assayed in duplicate. A *P* value of less than 0.05 was considered to be statistically significant. For the MTT assay, the data were normalized to cells grown in a standard tissue culture well and the results were expressed as percent viability. Significance level notation was expressed as \**P* < 0.05, \*\**P* < 0.01, and \*\*\**P* < 0.001.

## Conclusions

ZnO-coated nanoporous anodized aluminum oxide membranes were shown to produce significant cytotoxicity after 48 h in macrophages, a cell type involved in wound repair. It is possible to readily alter the thickness of a ZnO coating that is grown on a surface by means of ALD. Although the ZnO-coated membranes were noted to be cytotoxic (MTT assay) after 48 h, no statistically significant toxicity or ROS production was observed after 24 h. An exposure time longer than 24 h appears to be necessary to release a sufficient amount of Zn ions into media in order to produce an adverse cell response. A threshold Zn ion concentration for reduction in macrophage viability may exist, which was not reached after a 24 h exposure but was reached after additional exposure. Further studies are necessary to determine the optimal thickness of a ZnO coating on nanoporous surfaces that will produce an antimicrobial effect while minimizing cytotoxicity. Studies involving other cells of the immune system are also necessary to fully understand the potential in vivo cytotoxicity of ZnO-coated nanoporous anodized aluminum oxide membranes.

## Disclosure of Potential Conflicts of Interest

No potential conflicts of interest were disclosed.

## Acknowledgments and Support

P.E.P. is supported in part by NSF Award #1041375. Argonne is a US. Department of Energy Office of Science laboratory and is operated under Contract No. DE-AC02-06CH11357.

## Note

The mention of commercial products, their sources, or their use in connection with material reported herein is not to be construed as either an actual or implied endorsement of such products by the Department of Health and Human Services.

## References

- Leung YH, Chan CMN, Ng AMC, Chan HT, Chiang MWL, Djurišić AB, et al. Antibacterial activity of ZnO nanoparticles with a modified surface under ambient illumination. *Nanotechnology* 2012; 23:475703; PMID:23103840; <http://dx.doi.org/10.1088/0957-4484/23/47/475703>
- El-Hady MM, Farouk A, Sharaf S. Flame retardancy and UV protection of cotton based fabrics using nano ZnO and polycarboxylic acids. *Carbohydr Polym* 2013; 92:400-6; PMID:23218312; <http://dx.doi.org/10.1016/j.carbpol.2012.08.085>
- Lansdown ABG, Mirastschijski U, Stubbs N, Scanlon E, Agren MS. Zinc in wound healing: theoretical, experimental, and clinical aspects. *Wound Repair Regen* 2007; 15:2-16; PMID:17244314; <http://dx.doi.org/10.1111/j.1524-475X.2006.00179.x>
- Kumar PTS, Lakshmanan VK, Biswas R, Nair SV, Jayakumar R. Synthesis and biological evaluation of chitin hydrogel/nano ZnO composite bandage as antibacterial wound dressing. *J Biomed Nanotechnol* 2012; 8:891-900; PMID:23029997; <http://dx.doi.org/10.1166/jbn.2012.1461>
- Santimano MC, Kowshik M. Altered growth and enzyme expression profile of ZnO nanoparticles exposed non-target environmentally beneficial bacteria. *Environ Monit Assess* 2013; In press; PMID:23341058; <http://dx.doi.org/10.1007/s10661-013-3094-6>
- Premanathan M, Karthikeyan K, Jeyasubramanian K, Manivannan G. Selective toxicity of ZnO nanoparticles toward Gram-positive bacteria and cancer cells by apoptosis through lipid peroxidation. *Nanomedicine* 2011; 7:184-92; PMID:21034861; <http://dx.doi.org/10.1016/j.nano.2010.10.001>
- Song WH, Zhang JY, Guo J, Zhang JH, Ding F, Li LY, et al. Role of the dissolved zinc ion and reactive oxygen species in cytotoxicity of ZnO nanoparticles. *Toxicol Lett* 2010; 199:389-97; PMID:20934491; <http://dx.doi.org/10.1016/j.toxlet.2010.10.003>
- Andersson-Willman B, Gehrman U, Cansu Z, Buerki-Thurnherr T, Krug HF, Gabrielsson S, et al. Effects of subtoxic concentrations of TiO<sub>2</sub> and ZnO nanoparticles on human lymphocytes, dendritic cells and exosome production. *Toxicol Appl Pharmacol* 2012; 264:94-103; PMID:22842014; <http://dx.doi.org/10.1016/j.taap.2012.07.021>
- Kim YH, Fazlollahi F, Kennedy IM, Yacobi NR, Hamm-Alvarez SF, Borok Z, et al. Alveolar epithelial cell injury due to zinc oxide nanoparticle exposure. *Am J Respir Crit Care Med* 2010; 182:1398-409; PMID:20639441; <http://dx.doi.org/10.1164/rccm.201002-0185OC>
- Fukui H, Horie M, Endoh S, Kato H, Fujita K, Nishio K, et al. Association of zinc ion release and oxidative stress induced by intratracheal instillation of ZnO nanoparticles to rat lung. *Chem Biol Interact* 2012; 198:29-37; PMID:22640810; <http://dx.doi.org/10.1016/j.cbi.2012.04.007>
- Kumar PTS, Lakshmanan VK, Anilkumar TV, Ramya C, Reshmi P, Unnikrishnan AG, et al. Flexible and microporous chitosan hydrogel/nano ZnO composite bandages for wound dressing: in vitro and in vivo evaluation. *ACS Appl Mater Interfaces* 2012; 4:2618-29; PMID:22489770; <http://dx.doi.org/10.1021/am300292v>
- Leite-Silva VR, Lamer ML, Sanchez WY, Liu DC, Sanchez WH, Morrow I, et al. The effect of formulation on the penetration of coated and uncoated zinc oxide nanoparticles into the viable epidermis of human skin in vivo. *Eur J Pharm Biopharm* 2013; 84:297-308; PMID:23454052; <http://dx.doi.org/10.1016/j.ejpb.2013.01.020>
- Ostrowski AD, Martin T, Conti J, Hurt I, Harthorn BH. Nanotoxicology: characterizing the scientific literature, 2000-2007. *J Nanopart Res* 2009; 11:251-7; PMID:21170129; <http://dx.doi.org/10.1007/s11051-008-9579-5>
- Li T, Jia F, Fan Y, Ding Z, Yang J. Fabrication of nanoporous thin-film working electrodes and their biosensing applications. *Biosens Bioelectron* 2013; 42:5-11; PMID:23208085; <http://dx.doi.org/10.1016/j.bios.2012.10.003>
- Skoog SA, Bayati MR, Petrochenko PE, Staflieni S, Daniels J, Cilz N, et al. Antibacterial activity of zinc oxide-coated nanoporous alumina. *Mater Sci Eng B* 2012; 177:992-8; <http://dx.doi.org/10.1016/j.mseb.2012.04.024>
- Hoess A, Thormann A, Friedmann A, Heilmann A. Self-supporting nanoporous alumina membranes as substrates for hepatic cell cultures. *J Biomed Mater Res A* 2012; 100:2230-8; PMID:22492687
- Ferraz N, Hoess A, Thormann A, Heilmann A, Shen JH, Tang LP, et al. Role of alumina nanoporosity in acute cell response. *J Nanosci Nanotechnol* 2011; 11:6698-704; PMID:22103070; <http://dx.doi.org/10.1166/jnn.2011.4206>
- Manikandan E, Moodley MK, Sinha Ray S, Panigrahi BK, Krishnan R, Padhy N, et al. Zinc oxide epitaxial thin film deposited over carbon on various substrate by pulsed laser deposition technique. *J Nanosci Nanotechnol* 2010; 10:5602-11; PMID:21133080; <http://dx.doi.org/10.1166/jnn.2010.2478>
- Hsu JC, Lin YH, Wang PW, Chen YY. Spectroscopic ellipsometry studies on various zinc oxide films deposited by ion beam sputtering at room temperature. *Appl Opt* 2012; 51:1209-15; PMID:22441463; <http://dx.doi.org/10.1364/AO.51.001209>
- Pedersen JD, Esposito HJ, Teh KS. Direct synthesis and characterization of optically transparent conformal zinc oxide nanocrystalline thin films by rapid thermal plasma CVD. *Nanoscale Res Lett* 2011; 6:568; PMID:22040295; <http://dx.doi.org/10.1186/1556-276X-6-568>
- Zhao YL, Duan L, Dong GF, Zhang DQ, Qiao J, Wang L, et al. High-performance transistors based on zinc tin oxides by single spin-coating process. *Langmuir* 2013; 29:151-7; PMID:23210920; <http://dx.doi.org/10.1021/la304581c>
- Kayaci F, Ozgit-Akgun C, Donmez I, Biyikli N, Uyar T. Polymer-inorganic core-shell nanofibers by electrospinning and atomic layer deposition: flexible nylon-ZnO core-shell nanofiber mats and their photocatalytic activity. *ACS Appl Mater Interfaces* 2012; 4:6185-94; PMID:23088303; <http://dx.doi.org/10.1021/am3017976>
- Palomäki J, Karisola P, Pylkkänen L, Savolainen K, Alenius H. Engineered nanomaterials cause cytotoxicity and activation on mouse antigen presenting cells. *Toxicology* 2010; 267:125-31; PMID:19897006; <http://dx.doi.org/10.1016/j.tox.2009.10.034>
- Walpole AR, Xia ZD, Wilson CW, Triffitt JT, Wilshaw PR. A novel nano-porous alumina biomaterial with potential for loading with bioactive materials. *J Biomed Mater Res A* 2009; 90:46-54; PMID:18481790; <http://dx.doi.org/10.1002/jbm.a.32067>
- Nagy A, Harrison A, Sabbani S, Munson RS Jr., Dutta PK, Waldman WJ. Silver nanoparticles embedded in zeolite membranes: release of silver ions and mechanism of antibacterial action. *Int J Nanomedicine* 2011; 6:1833-52; PMID:21931480
- McDevitt CA, Ogunniyi AD, Valkov E, Lawrence MC, Kobe B, McEwan AG, et al. A molecular mechanism for bacterial susceptibility to zinc. *PLoS Pathog* 2011; 7:e1002357; PMID:22072971; <http://dx.doi.org/10.1371/journal.ppat.1002357>
- Bozym RA, Chimenti F, Giblin LJ, Gross GW, Korichneva I, Li YA, et al. Free zinc ions outside a narrow concentration range are toxic to a variety of cells in vitro. *Exp Biol Med (Maywood)* 2010; 235:741-50; PMID:20511678; <http://dx.doi.org/10.1258/ebm.2010.009258>
- Heng BC, Zhao XX, Xiong SJ, Ng KW, Boey FYC, Loo JSC. Cytotoxicity of zinc oxide (ZnO) nanoparticles is influenced by cell density and culture format. *Arch Toxicol* 2011; 85:695-704; PMID:20938647; <http://dx.doi.org/10.1007/s00204-010-0608-7>
- von Bülow V, Dubben S, Engelhardt G, Hebel S, Plümackers B, Heine H, et al. Zinc-dependent suppression of TNF-alpha production is mediated by protein kinase A-induced inhibition of Raf-1, I kappa B kinase beta, and NF-kappa B. *J Immunol* 2007; 179:4180-6; PMID:17785857
- Grandjean-Laquerriere A, Laquerriere P, Jallot E, Nedelec JM, Guenounou M, Laurent-Maquin D, et al. Influence of the zinc concentration of sol-gel derived zinc substituted hydroxyapatite on cytokine production by human monocytes in vitro. *Biomaterials* 2006; 27:3195-200; PMID:16487585; <http://dx.doi.org/10.1016/j.biomaterials.2006.01.024>
- Chvapil M, Ryan JN, Elias SL, Peng YM. Protective effect of zinc on carbon tetrachloride-induced liver injury in rats. *Exp Mol Pathol* 1973; 19:186-96; PMID:4754789; [http://dx.doi.org/10.1016/0014-4800\(73\)90078-6](http://dx.doi.org/10.1016/0014-4800(73)90078-6)
- Waalkes MP, Rehm S, Riggs CW, Bare RM, Devor DE, Poirier LA, et al. Cadmium carcinogenesis in male Wistar [CrI:(WI)BR] rats: dose-response analysis of effects of zinc on tumor induction in the prostate, in the testes, and at the injection site. *Cancer Res* 1989; 49:4282-8; PMID:2743314
- Floersheim GL. Protection against acute ethanol toxicity in mice by zinc aspartate, glycyls, levulose and pyritinol. *Agents Actions* 1985; 16:580-4; PMID:4072834; <http://dx.doi.org/10.1007/BF01983665>
- Floersheim GL, Floersheim P. Protection against ionising radiation and synergism with thiols by zinc aspartate. *Br J Radiol* 1986; 59:597-602; PMID:3518853; <http://dx.doi.org/10.1259/0007-1285-59-702-597>
- Rostan EF, DeBuys HV, Madey DL, Pinnell SR. Evidence supporting zinc as an important antioxidant for skin. *Int J Dermatol* 2002; 41:606-11; PMID:12358835; <http://dx.doi.org/10.1046/j.1365-4362.2002.01567.x>